Supplemental Material

Reduction in Kv Current Enhances the Temporal Dispersion of the Action Potential in Diabetic Myocytes: Insights from a Novel Repolarization Algorithm

Meo et al

Material and Methods

Newly Developed Repolarization Analysis

A signal processing method previously used for ECG recordings[1] was adapted for the analysis of action potentials (APs). Briefly, Axon binary files containing a sequence of APs in the form of sequential sweeps were converted into text files. Subsequently, data were imported in Matlab (MathWorks) software as matrices with size *b x S*, where *b* is the number of sequential sweeps (APs) and *S* is the number of samples collected during each sweep. Each repolarization phase of the AP was modeled using the following steps: *i*) segmentation of the repolarization phase of the AP and normalization of the AP amplitude in the interval [0-1]; *ii*) fitting of repolarization segments (intervals) based on least square approximation, subjected to monotonically decreasing behavior constraints;[1] and *iii*) interpolation of the reciprocal functions of the obtained fitting over a fixed range of the AP repolarization.

We considered the acquisition x_i of the ith repolarization interval for a given sequence of APs relative to a myocyte uniformly sampled over the time, with the variable n being the sample index. The computation of the reciprocal function imposes that observations are strictly decreasing or increasing. In the case of the rodent AP, the strictly decreasing behavior of the repolarization was considered and modeled using a parametric function f, characterized by the parameter vector $\boldsymbol{\theta}_i$, which is different for each repolarization. Thus, the ith sampled repolarization was modeled using the following:

$$x_i(n) = f(n; \boldsymbol{\theta}_i) + e_i(n)$$

where $n = 1, \cdots, N$ and $e_i(n)$ accounts for the acquisition and noise modeling. More specifically, $f(n; \boldsymbol{\theta}_i)$ is a piecewise linear parametric function defined as a weighted sum of a collection of functions $v_l(n)$:

$$f(n; \boldsymbol{\theta}_i) = \sum_{l=1}^{L} \theta_i[l]\, v_l(n)$$

We built a collection of L functions $v_l(n)$ which defines L intervals of width K.[1] In this application the interval length was chosen as 3, L is the largest integer not greater than $(N+1)/2$ and N was assumed as an odd number (see example reported in Figure S8). As previously reported,[1] imposing $f(n; \boldsymbol{\theta}_i)$ to be strictly decreasing is equivalent to verify the condition:

$$\forall l \in [1: L-1], \theta_i[l] > \theta_i[l+1] > 0$$

Then, the least square estimation of $\boldsymbol{\theta}_i$ was performed according to following constraint:

$$\widehat{\boldsymbol{\theta}}_i = \arg\min_{\boldsymbol{\theta}_i} \sum_{n=1}^{N} (x_i(n) - f(n; \boldsymbol{\theta}_i))^2$$

The estimation method is a linear-inequality constraints problem (LSI problem) converted in a least distance programming (LDP) problem.[2] Once the estimation was computed, $x_i(n)$ was replaced by $f(n; \widehat{\boldsymbol{\theta}}_i)$ for subsequent calculation. The process originated a decreasing function that allowed filtering of acquisition noise, accounted by $e_i(n)$ (see simulation reported in Figure S9).

The imposed decreasing property of the function $f(n; \boldsymbol{\theta}_i)$ led to the computation of a unique value for n from the reciprocal function $n = f^{-1}(y, \boldsymbol{\theta}_i)$ for any given value of y. Repolarization levels relative to the normalized amplitude of the AP were initially reported on the horizontal axis, whereas corresponding values for duration of repolarization were reported on the vertical axis. In order to compare the entire set of APs, regardless of the stimulation index ith, identical repolarization levels were obtained, by interpolating $f^{-1}(y, \boldsymbol{\theta}_i)$ over a fixed set of y values.

For each myocyte, the obtained values of duration of repolarization segments for sequential APs computed with the algorithm were then employed to calculate average AP profile and degree of beat-to-beat variability. Parameters obtained in each cells were then used to compute average AP profile for control myocytes, STZ-myocytes and for cells before and after exposure to 4-AP. Similarly, fold change and statistical comparison between two experimental groups were calculated. Repolarization properties were graphically visualized using Prism software, with repolarization levels on the y axis and repolarization time on the x axis.

References

1. Cabasson A, Meste O, Blain G and Bermon S. Quantifying the PR interval pattern during dynamic exercise and recovery. *IEEE Trans Biomed Eng*. 2009;56:2675-83.
2. Lawson CL and Hanson RJ. *Solving least squares problems*. Englewood Cliffs, N.J.,: Prentice-Hall; 1974.

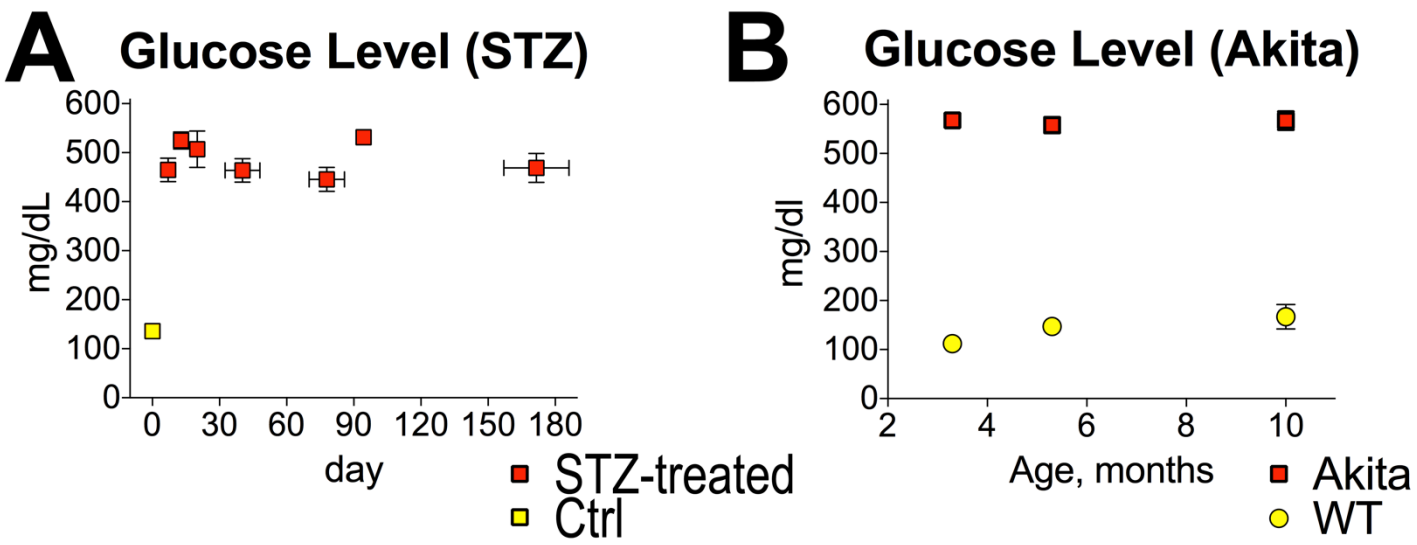

Figure S1. Blood glucose in control and diabetic mice. **A,** Circulating glucose levels in non-treated (0 days) and STZ-treated female mice as a function of time from treatment. Data are shown as mean±SEM (n=7-30 mice for each time point). **B,** Circulating glucose levels in wild-type (WT) and Akita male mice as a function of age. Data are shown as mean±SEM (n=4-7 mice for each time point).

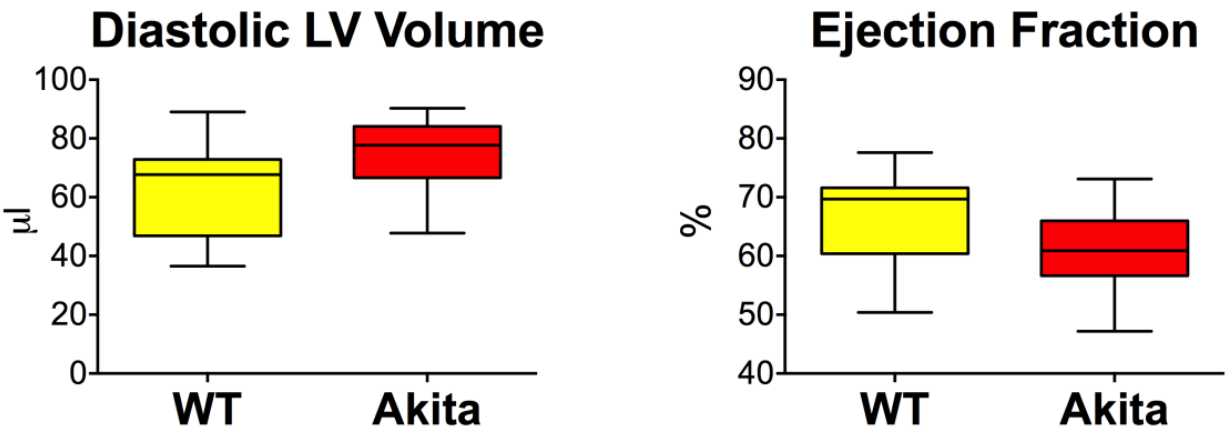

Figure S2. Cardiac function in Akita mice. Quantitative data obtained by echocardiography in male wild-type (WT; n=7) and Akita (n=8) mice at ~7 months of age are shown as median and interquartile ranges (IQR).

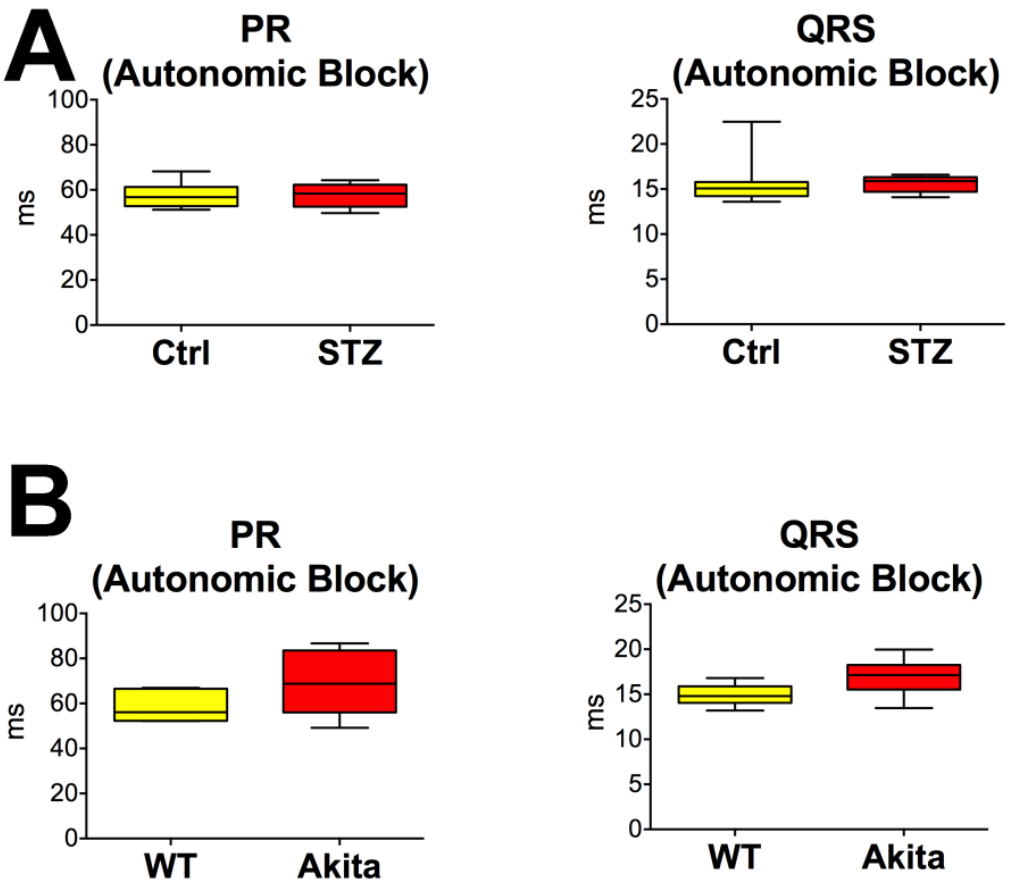

Figure S3. Hyperglycemia and electrocardiographic parameters under complete autonomic block. **A** and **B,** Additional electrocardiographic parameters in Ctrl and STZ female mice (**A**) and WT and Akita (**B**) male mice reported in Figure 3D and 3E, are shown as median and IQR.

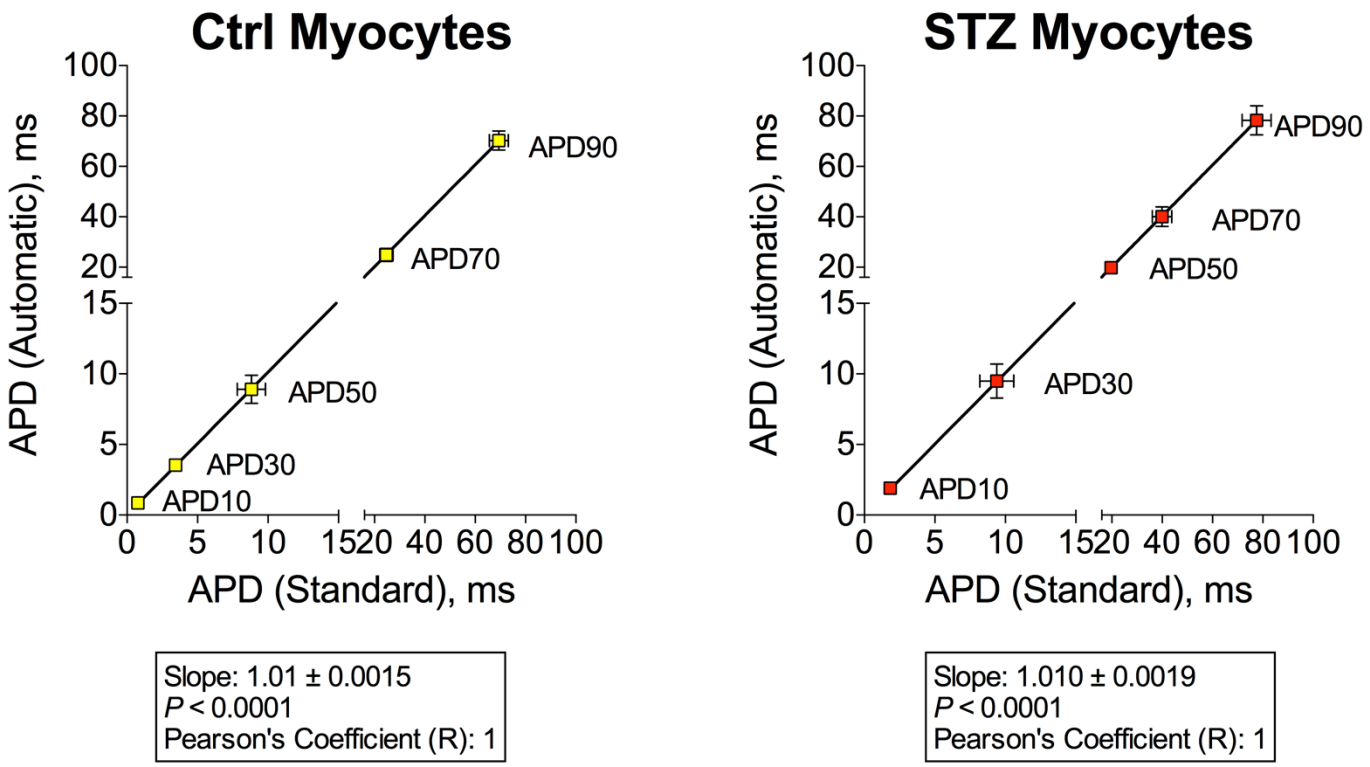

Figure S4. Comparison of AP parameters obtained by standard analysis and the novel algorithm. Relation between AP duration at discrete repolarization levels computed with conventional (Standard) and newly developed (Automatic) approaches. Data obtained in Ctrl and STZ myocytes shown in Figure 5B and 5C are reported as mean±SEM and are fitted with linear regression.

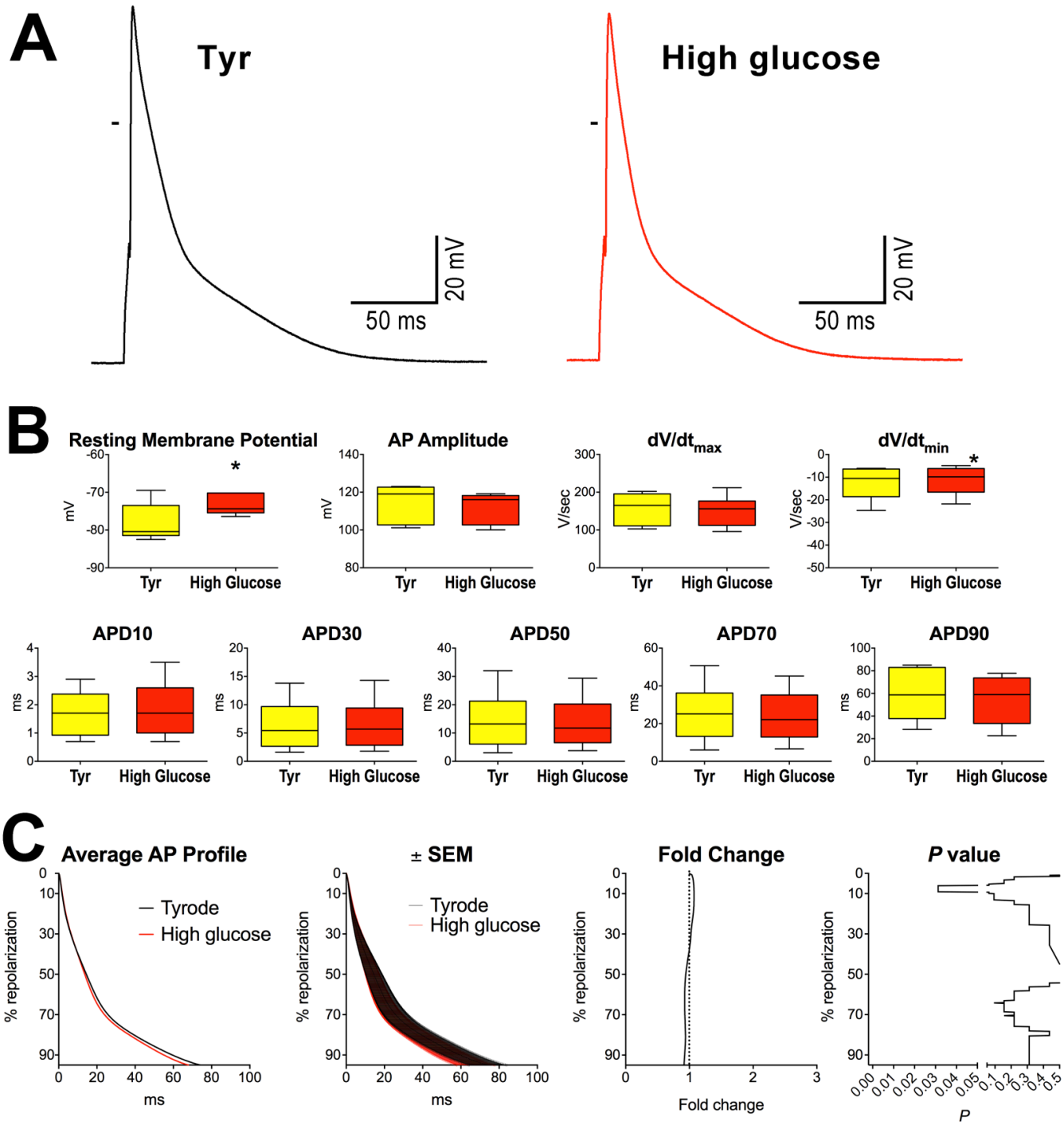

Figure S5. High glucose and AP profile. **A,** APs obtained in a myocytes from a Ctrl female mouse heart before and following exposure to 20 mmol/L glucose (High glucose). **B**, AP properties of Ctrl myocytes (n=6 from 3 female mice) stimulated at 1 Hz before (Tyr) and after exposure to 20 mmol/L glucose (High Glucose) are shown as median and IQR. **P*<0.05 versus Tyr. **C,** Analysis and comparison of repolarization properties of APs reported in **B** using the novel algorithm. Graph of Average AP Profile represents the calculated average repolarization phase of the AP in myocytes before and after exposure to 20 mmol/L glucose. Corresponding error bars, fold changes for the duration of the AP in high glucose versus Tyrode and statistical difference are reported in the ±SEM, Fold Change and *P* value graphs, respectively.

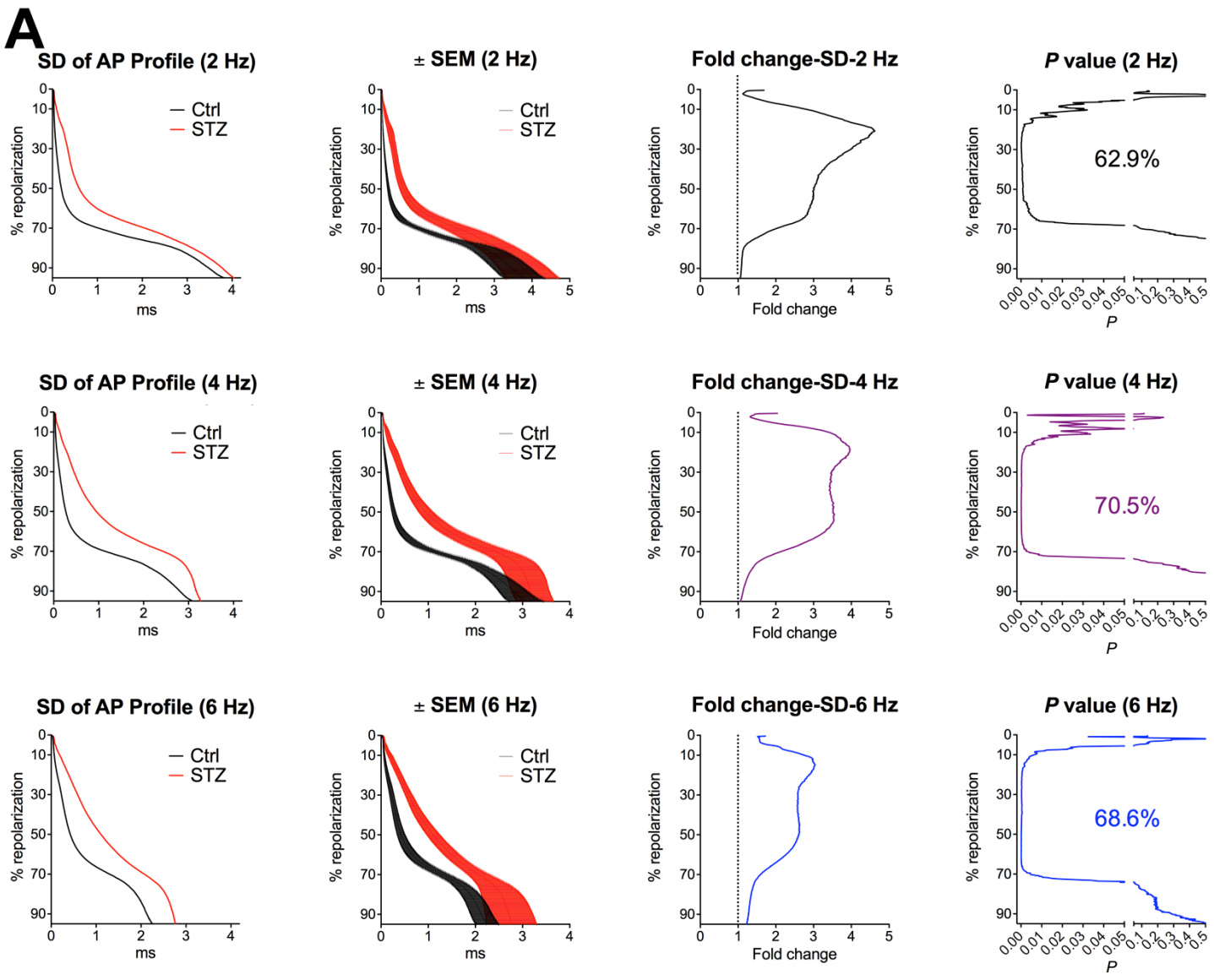

Figure S6. Hyperglycemia and AP properties at different pacing rates. **A** through **C,** Variability of the repolarization of the AP at 2, 4 and 6 Hz pacing rates evaluated by SD (**A**), RSD (**B**) and STV (**C**) using the novel algorithm for cells reported in Figure 6. Graphs of SD, RSD and STV of AP Profile represent the calculated average variability of the repolarization phase of the AP for Ctrl and STZ myocytes. Corresponding error bars, fold changes for the variability of the AP in STZ versus Ctrl cells and statistical difference are reported in the ±SEM, Fold Change and *P* value graphs, respectively.

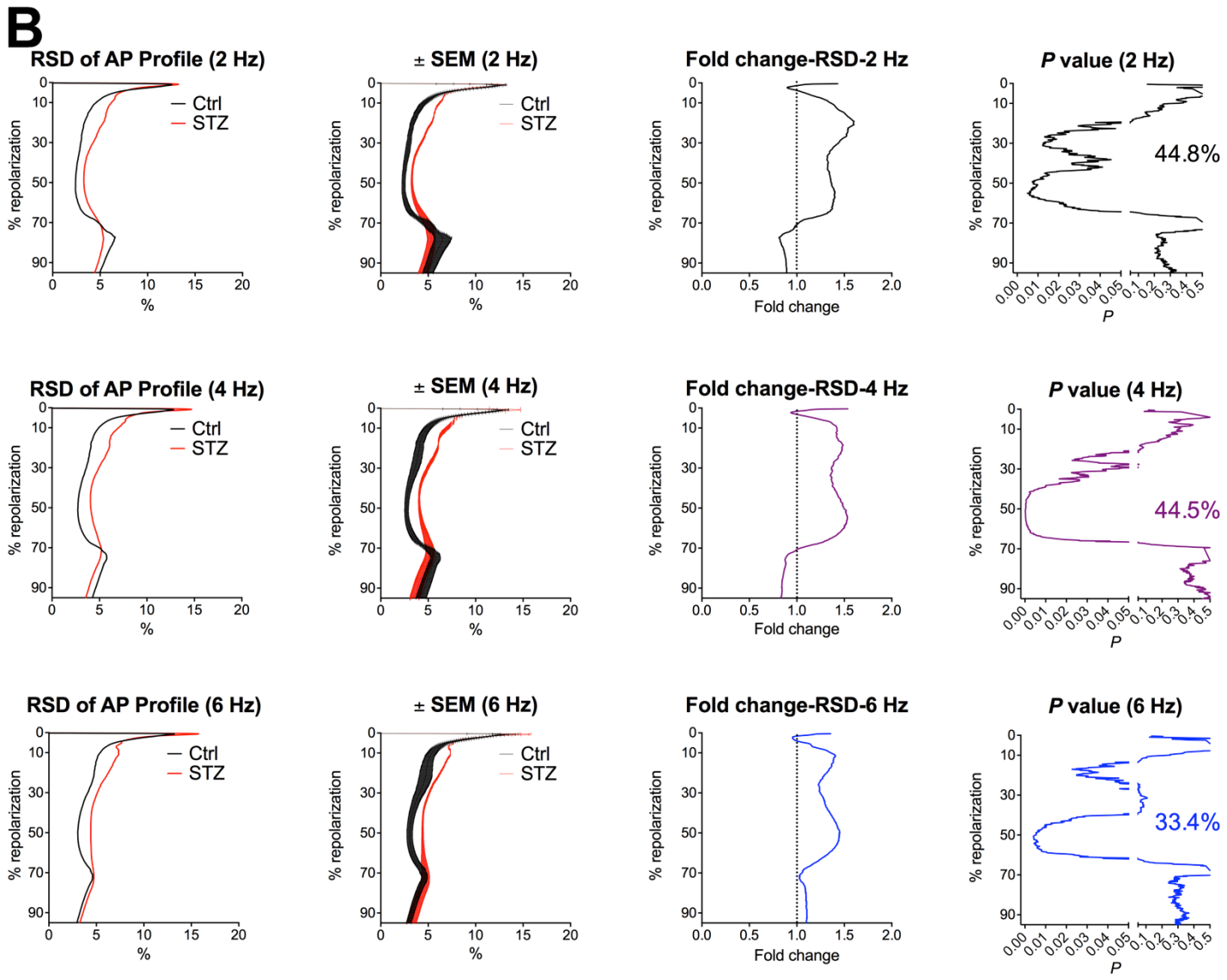

Figure S6. (Continued).

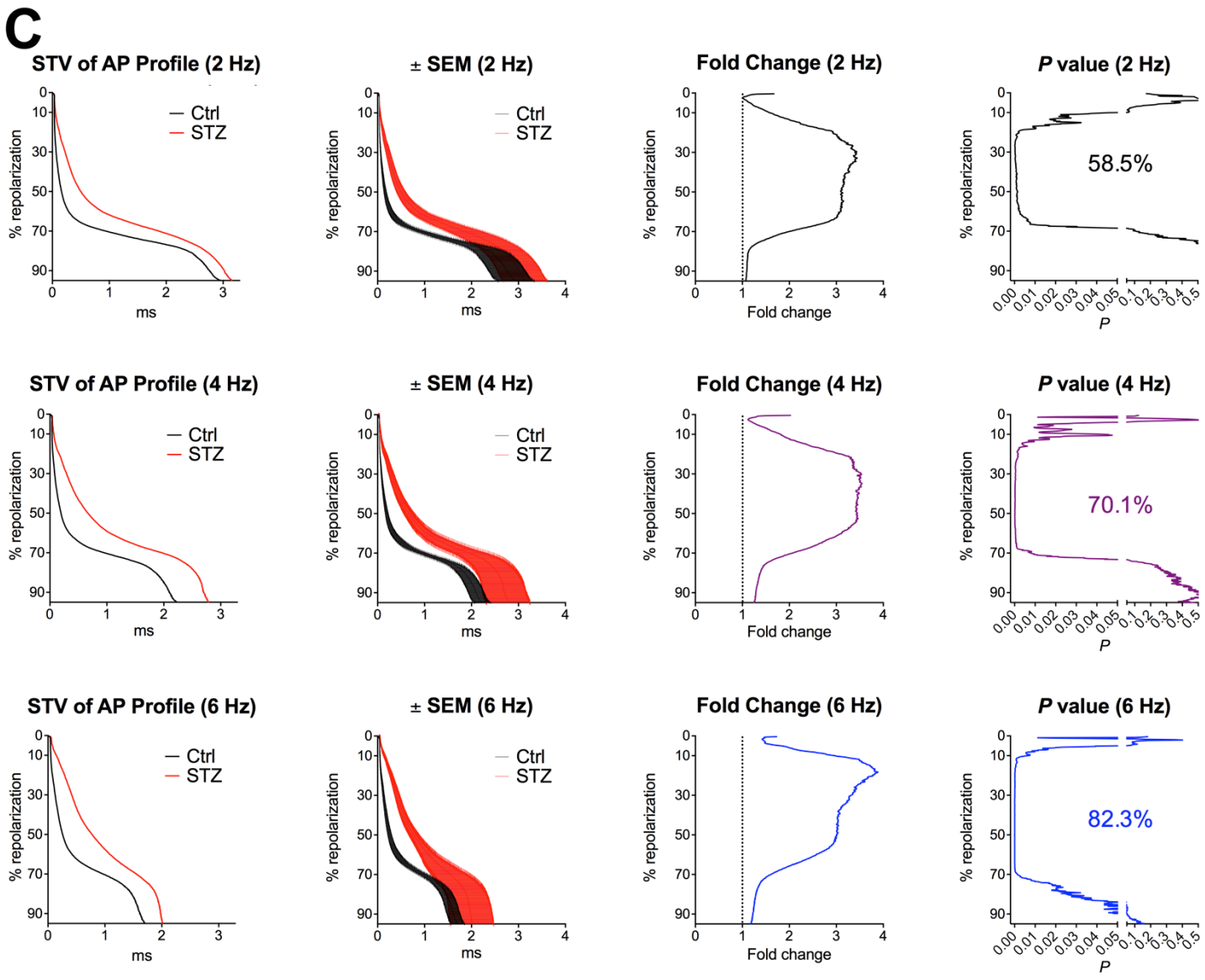

Figure S6. (Continued).

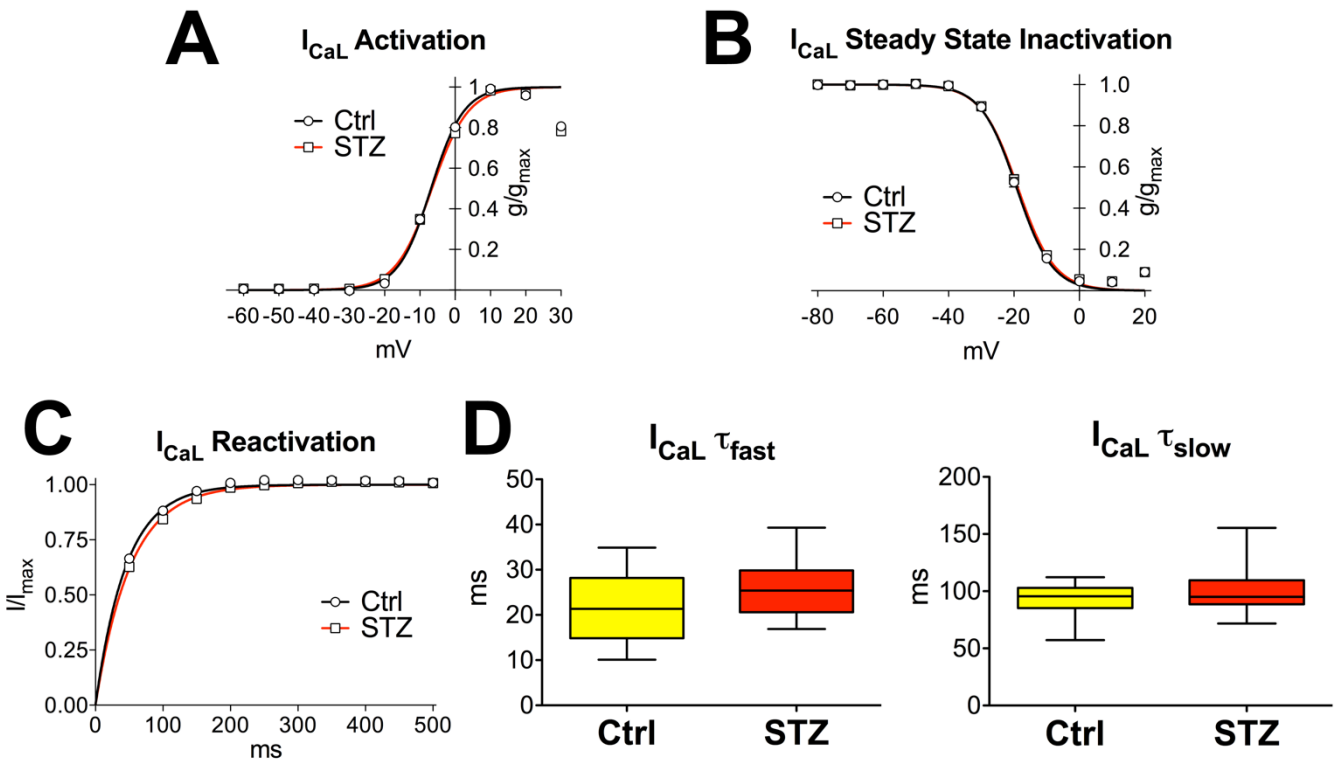

Figure S7. Hyperglycemia and I_{CaL} properties. **A,** Activation curves of I_{CaL} for Ctrl myocytes (n=21, from 3 mice) and myocytes from STZ-treated female mice (n=22, from 4 mice at 12-19 days following the induction of diabetes) are shown as mean±SEM. Fitting parameters: Ctrl: $V_{1/2G}$ -6.8±0.3 mV, k_G 4.6±0.3 mV, R^2 0.96; STZ: $V_{1/2G}$ -6.6±0.3 mV, k_G 5.2±0.3 mV, R^2 0.96. **B,** Steady state inactivation curves of I_{CaL} for Ctrl myocytes (n=21, from 3 mice) and myocytes from STZ-treated mice (n=19, from 4 mice at 12-19 days following the induction of diabetes) are shown as mean±SEM. Fitting parameters: Ctrl: $V_{1/2G}$ -19.2±0.2 mV, k_G 5.4±0.2 mV, R^2 0.99; STZ: $V_{1/2G}$ -18.8±0.2 mV, k_G 5.6±0.2 mV, R^2 0.99. . **C,** Recovery from inactivation curves of I_{CaL} for Ctrl myocytes (n=15, from 3 mice) and myocytes from STZ-treated mice (n=16, from 4 mice at 12-19 days following the induction of diabetes) are shown as mean±SEM. Fitting parameters: Ctrl: τ 45.4±1 ms, R^2 0.88; STZ: τ 51.9±1 ms, R^2 0.91. **D,** Inactivation time constants of I_{CaL} for Ctrl myocytes (n=20, from 3 mice) and myocytes from STZ-treated mice (n=17, from 4 mice at 12-19 days following the induction of diabetes) are shown as median and IQR.

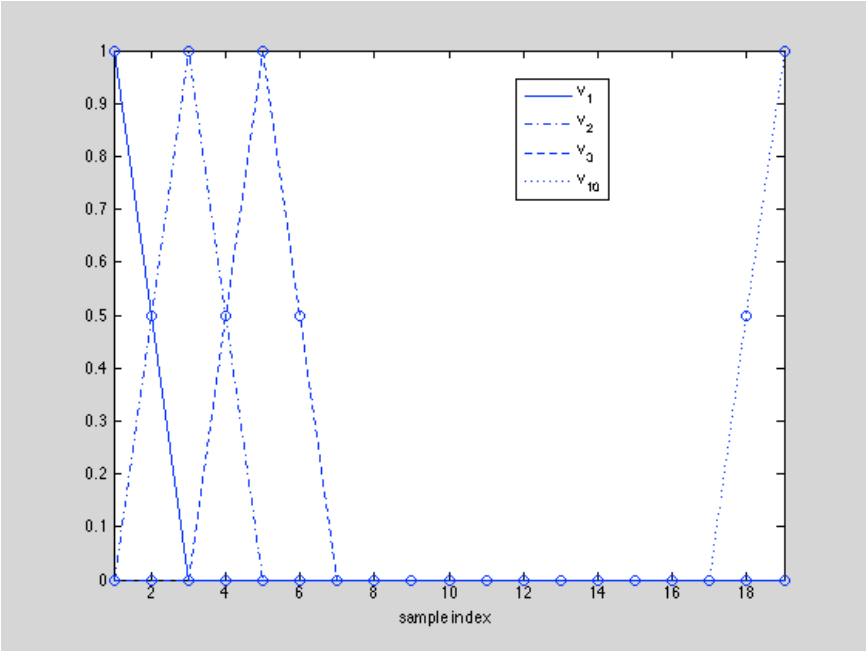

Figure S8. Novel algorithm. Example of a collection of $v_l(n)$ functions when considering $N = 19$, thus leading to $L = 10$. Vectors are represented by small circles.

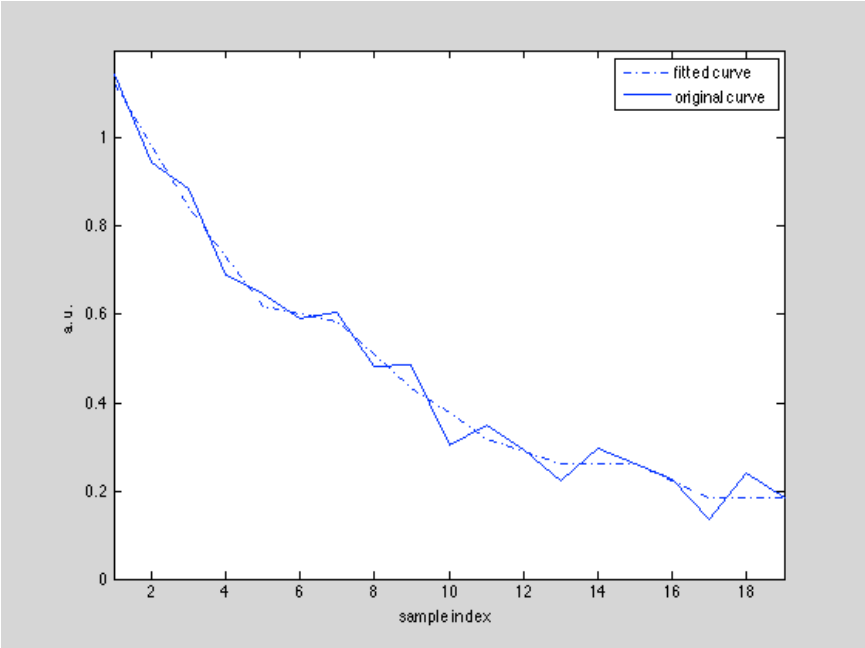

Figure S9. Novel algorithm. Simulated 19-samples signal of the repolarization phase of the AP and resulting fitted curve. Fitted curve is smooth with respect to original signal and exhibit monotonic decay.